PASSIVE EMBEDDED SENSOR FOR DETECTING BONE INTEGRATION IN ORTHOPEDIC IMPLANTS

by

TULSI PATEL

A THESIS

Presented to the Department of Human Physiology
and the Robert D. Clark Honors College
in partial fulfillment of the requirements for the degree of
Bachelor of Science

May 2024

An Abstract of the Thesis of

Tulsi Patel for the degree of Bachelor of Science
in the Department of to be taken June 2024

Title: Passive Embedded Sensor for Detecting Bone Integration in Orthopedic Implants

Approved: *Keat Ghee Ong, Ph.D.*
Primary Thesis Advisor

The rate of orthopedic implant failures has increased in the last few decades, raising medical costs for treatment and rehabilitation of these failures from $320 million to $566 million in less than a decade. The clinical outcomes of orthopedic implants have improved with the rapid advancement in new materials and surface modifications for implants that enhance bone integration with implant, thus increasing stability while reducing the rate of implant failure. However, determining and monitoring this bone-implant integration quantitatively has been a challenge as the current method of micro-CT scans are slow, tedious, and provide little insight. This project's goal is to design a tool that can track bone-implant integration after spinal fusion surgery (surgery in which an implant is inserted between two vertebral discs to promote the fusion of those two discs, often after traumatic injury in that area), which can be vital for personalized and timely patient care to reduce revision surgeries and improve rehabilitation. The wireless and passive sensor is meant to be incorporated into a porous PEEK surface, a common material used in orthopedic implants, to detect bone growth in the extremity of implants such as spinal cages. The sensor was based on an inductive-capacitive resonance circuit that can be remotely interrogated with an external device to monitor localized bone growth and mineralization. Preliminary results using modified simulated body fluid (a solution that can

mimic bone formation/mineralization) have shown significant decreases in the resonance frequency (an inherent frequency emitted by the sensor) as bone mineralization increases. Further aspects of this study will continue to analyze the effects of other parameters, such as temperature, bone density, and cell growth.

Acknowledgements

I would like to thank Dr. Keat Ghee Ong and Dr. Salil Karipott for being incredible mentors throughout my time in the Ong Lab. When I entered the lab as a freshman, all I knew was that I wanted to contribute to a project that was meaningful not only to me but to a wider community. Their tireless support and guidance through all the ups and downs of this project has been the most incredible gift and I am truly grateful to them. I am immensely grateful to Dr. Brian McWhorter for his amazing support and insight. His sense of humor and wisdom were incredibly helpful during the most stressful moments of this process.

I would like to thank my parents for always pushing me to do my best no matter what. I would not be who I am today without them and their continuous support and love.

TABLE OF CONTENTS

List of Tables/Graphs/Illustrations

I. INTRODUCTION

Orthopedics is a branch of medicine related to correcting deformities and disorders of bones and muscles (American Board of Orthopaedic Surgery, 2019). An orthopedic implant is a medical device designed to replace a missing joint or bone or to support a damaged bone (Center for Orthopedic Surgery and Sports Medicine, 2019). Orthopedic implants have a variety of applications and can be used in many locations within the body, including the teeth, hip joint, and the spine. Orthopedic implants promote bone growth through the implant, allowing integration between the implant and the tissue surrounding the implant. This allows the body to work with the implant in reinstating or improving normal functions of the body. However, orthopedic implants are often associated with a high incidence of infections in the site of implantation (Karipott et. al., 2018). According to an analysis of a survey performed by Agency for Healthcare Quality and Research, 2.0 to 2.4% of knee and hip replacement surgeries performed in 2001 and 2009 were associated with an infection at the implantation site, resulting in an increase from $320 million to $566 million expenditure for medical treatment and rehabilitation (Kurtz et. al., 2012). Untreated or late treatment of infection can result in complications including implant rejection and amputation (Karipott et. al., 2018). Unfortunately, there are no accurate and insightful methods of detecting and monitoring tissue-implant integration of orthopedic implants. In most current cases, physicians will utilize CT or x-ray scans to provide some visual of the integration, but these scans are tedious and provide little insight due to poor spatial resolution (Karipott et. al., 2018) (Liu et al., 2011).

Passive embedded wireless sensors are meant to provide non-invasive and accurate monitoring of bone integration that can catch bone implant failure early on to prevent worse situations such as implant rejection or amputation. Though orthopedic implants vary in size,

surface modifications, material, and function–thus posing the challenge of designing a sensor that can be adapted to such differences– the sensors can be manufactured and integrated into existing implant designs, allowing clinicians to monitor tissue-implant integration with ease and accuracy. Previous researchers have developed passive wireless sensors that have been shown to adapt to different environments, thus tracking changes relating to the orthopedic implant (Ong et. al., 2001). Passive embedded wireless sensors demonstrated potential usage in a variety of applications, including temperature, humidity, pressure, and biochemical sensing (Ong et. al., 2001). Thus, there are multiple dimensions to passive sensors that can account for the complexity of monitoring a complex physiology environment as is found with orthopedic implants.

II. SENSOR DESIGN

The inductive-capacitive (LC) sensor in this study was fabricated using FR4, a glass fiber-filled composite that is typically used as a backing material for manufacturing electronic circuits. A planar spiral pattern made of conductive copper metal is fabricated on the FR4 material (OSHPark) 10 mm in diameter and XX turns. The pattern was designed using electronics CAD software, Eagle (Autodesk). The sensors were coated in parylene-C, a chemically inert and biocompatible polymer that serves as a conformal coating providing electrical insulation for the conductive patterns (Tan & Craighead, 2010). The sensors were also treated with plasma O_2 etching, a process that uses oxygen gas plasma to etch the surface of organic materials. The plasma etching process makes the surface more hydrophilic.

a. Sensing Mechanism

The sensor designed in this research study is based on a resonant inductor-capacitor circuit (LC circuit or LC sensor). An LC circuit is a closed-loop system composed of two elements: a capacitor and an inductor (*LC Circuits*). A capacitor temporarily stores electrical energy through distributing charged particles across two plates to create an electric field, while an inductor stores and dissipates energy within its magnetic field. When a capacitor and inductor are connected in a closed-loop circuit, they can transfer energy back and forth between capacitors' electric field and inductors magnetic field as electric current flows, much like a pendulum where energy is transferred from kinetic to potential energy. The energy transfer is time dependent and at a specific frequency known as the resonance frequency the energy transfer in the system is the maximum. The Q factor or quality factor is the ratio of the resonance frequency over the bandwidth, a measure of the damping in the oscillating/resonating systems. In LC sensors and circuits resonant frequencies and Q factors can be used to detect change in inductive, capacitive and resistive parameters of the circuit. The basic sensing mechanism is based on the implication that the resonance frequency and/or the Q factor will change based on changes to the capacitance, inductance, and/or coupling distance (Huang et al., 2016).

LC sensors have been shown to monitor multiple physiological environments and multiple parameters such as temperature, humidity, and pressure (Karipott et al., 2017) (Li et al., 2021) (Khan et al., 2021). The purpose of this study is to determine the effect of bone like mineral deposition on an LC sensor and whether such deposition can be detected through changes in the resonance frequency and/or Q factor. In theory, this sensor would be manufactured into an orthopedic implant. When bone mineralizes within the orthopedic implant, it will mineralize between the conductive patterns of the LC sensor embedded into the implant.

Thus, as bone mineralizes onto the surface of the sensor, there is a change to the capacitance of the sensor which changes the resonance frequency of the sensor (Karipott et. al., 2018). This change in resonance frequency can be detected by an external readout coil to monitor bone growth through the orthopedic implant. This is similar to how a barcode scanner can be used to scan a barcode which stores information about an object.

III. METHODS

The LC sensor was tested using a Vector Network Analyzer (VNA) controlled by a custom computer program. The VNA is set up to measure reflection coefficient or S11 parameter with an external reader coil. When the coil is in range with the sensor to inductively couple, the measured S11 parameter of the reader coil will be a combination of both the sensor and the reader coil. All tests described below were conducted using the same measurement settings.

a. Temperature Testing

Temperature testing is necessary for this sensor as it determines the effect of temperature on the resonance frequency of the sensor. Temperature changes can cause thermal expansion and temperature-related resistance changes in the sensor. A controlled temperature test was conducted to evaluate changes in resonance frequency and Q factor of the sensor.

An incubator (ThermoFischer) was set up next to the VNA. The external readout coil was placed inside the incubator along with the sensors for measurements. Temperature was varied in the 32°C to 42°C range while measurements were recorded from the VNA with simultaneous temperature measurements recoded with an infrared thermometer.

b. Phosphate-buffered Saline Testing

Phosphate-buffered saline (PBS) is a pH buffer solution composed of different salts dissolved in water. These salts include sodium chloride, potassium chloride, potassium dihydrogen phosphate, and disodium hydrogen phosphate.

For the 24-hour PBS test, the VNA was set and calibrated to test parameters. A 20 mL glass vial was filled with 10 mL of PBS. Each sensor was placed inside the glass vial using tweezers, sealed, and then placed inside the incubator set to 37 °C. Each vial was set within the external readout coil inside the incubator with a measurement taken at the set interval of every half hour.

c. Modified Simulated Body Fluid Testing

Modified Simulated Body Fluid (mSBF) is an ion/mineral-rich solution which, when put under physiological temperatures, will precipitate to form an apatite structure similar to bone mineralization (Torstrick et. al., 2017). It is commonly used to simulate bone formation/mineralization and widely used in bone regeneration/remodeling research (Baino et. al., 2020).

For a 4× solution of simulated body fluid (mSBF), the amounts of minerals/salts are as follows: 16.4875 g of NaCl, 0.6225 g of KCl, 0.1255 g of $MgSO_4$, 0.409 g of $MgCl_2$, 0.709 g of $NaHCO_3$, 0.739 g of $CaCl_2$, 0.274 g of KH_2PO_4, and 1.9715 g of Tris-HCl. Place a clean 1000 mL beaker on a magnetic stir plate pH and adjust using 1 M NaOH and 1 M HCl to titrate the mSBF solution to the desired pH of 6.4.

In the 24-hour mSBF test, we are determining if the sensor can track an increase in mineralization upon the surface of the sensor. For the 24-hour SBF test, a 20 mL glass vial was filled with 10 mL of mSBF. One sensor was placed within the glass vial carefully. The incubator

temperature was set to 37°C. The coil was placed inside the incubator and allowed to obtain the background measurement. Once obtained, the vial was placed inside the incubator inside the coil in succession and measurements were taken at set time intervals.

In the 24-hour mSBF versus PBS test, we are determining if the changes seen in the 24-hour mSBF test are unique to SBF and not to other mineral-based solutions. Thus, PBS was used as a control basis to see if the resonance frequency of the sensor would change when in PBS as opposed to changes seen in mSBF.

IV. RESULTS

a. *Sensor Response in Air*

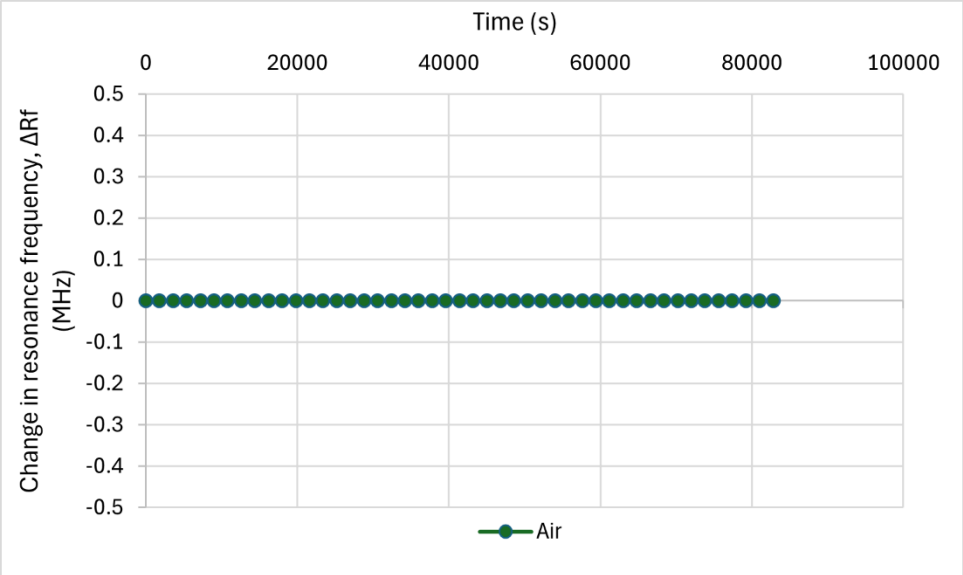

Figure 1: LC sensor response to air at room temperature (25°C).

As shown in Figure 1, the resonance frequency of the sensor does not change across the 24-hour period. The plot shows changes relative to the baseline resonance frequency.

b. Sensor Response to Temperature

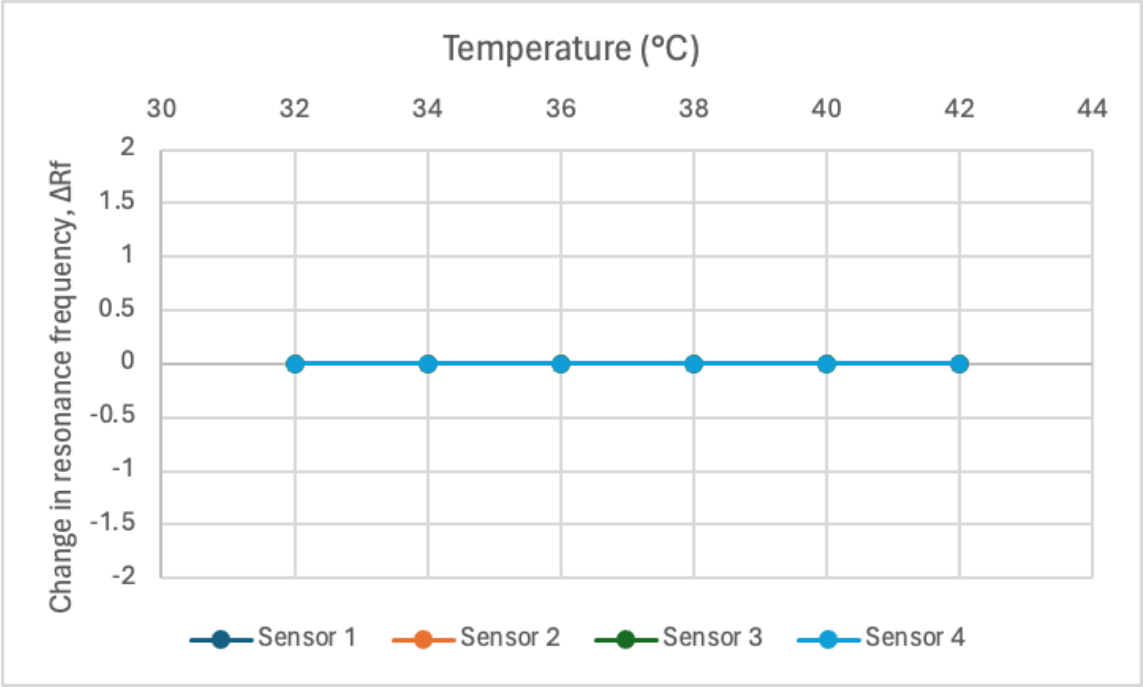

Figure 2: LC sensor response measured by resonance frequency due to change in temperature (°C)

Figure 2 shows change in resonance frequency due to change in temperature. The temperature range for this experiment was 32°C to 42°C with intervals of 2°C. As shown in Figure 2, there are no perceivable changes in the resonance frequency with temperature as it remains at a constant resonance frequency.

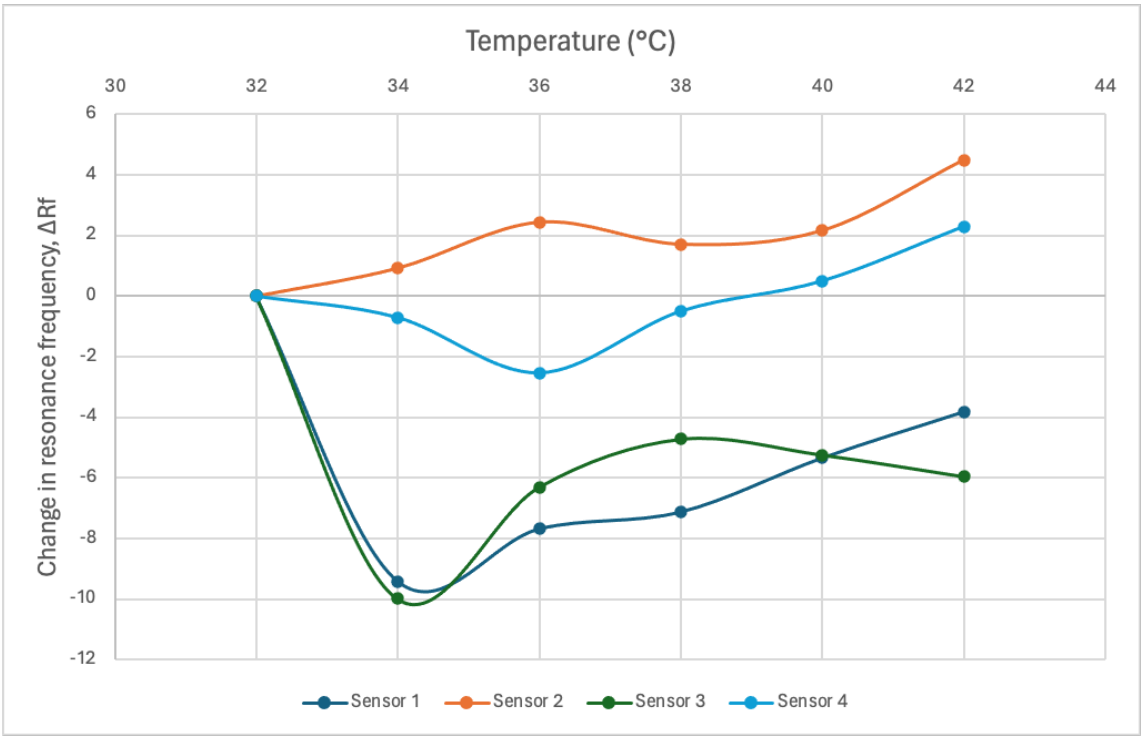

Figure 3: LC sensor response measured by Q factor due to change in temperature (°C)

Figure 3 describes the change in the Q factor of the LC sensor in response to the change in the temperature. All measurements were held relative to the starting resonance frequency for each sensor at 32°C, thus illustrating the change in resonance frequency over a 24-hour period.

c. Phosphate-buffered Saline versus Modified Simulated Body Fluid Response

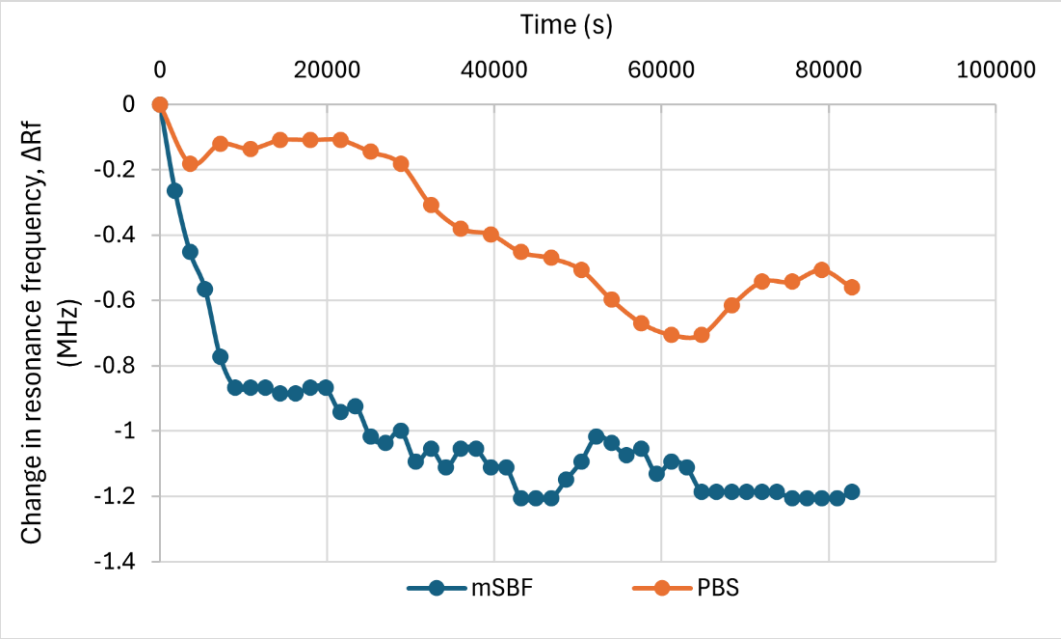

Figure 4: LC sensor response to PBS and 4x mSBF over a 24-hour period

As shown in Figure 4, 4x mSBF produces a steep decrease in resonance frequency in the first 3 hours as the crystallization of the salts occur in the saturated mSBF solution. Each data point is a rolling average of the sensor response measured from the sensor and resonance change is calculated as the difference from starting resonance frequency.

In Figure 4, the resonance frequency in response to mSBF decreases over the 24-hour period, eventually reaching a plateau after approximately 5 hours. There are some variations in the resonance frequency after this point, but the resonance frequency remains relatively stable. In comparison, the resonance frequency in response to PBS also decreases over the 24-hour period but to a lesser extent and does not reach a plateau.

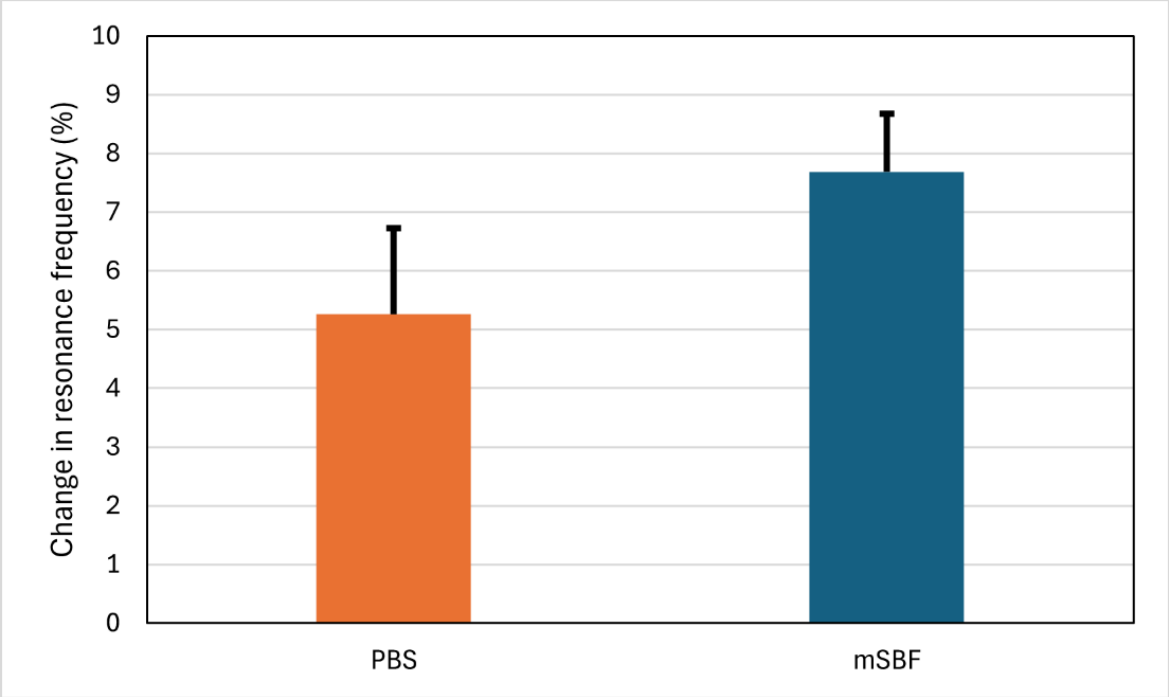

Figure 5: LC sensor's change in resonance frequency compared between PBS and mSBF

Figure 5 demonstrates the difference in the percent change in resonance frequency due to salts precipitating out of solution in either PBS or mSBF. It shows that mSBF has a greater percent change in resonance frequency than PBS.

V. DISCUSSION

a. Sensor Response in Air

As described in Figure 1, the resonance frequency of the LC sensor did not change over 24 hours at room temperature. Given that none of the parameters mentioned (such as inductance, capacitance, and coupling distance) did not change, the findings of no change in the resonance frequency is consistent with the lack of change in the environmental and sensor parameters. It is also promising that the sensor's resonance frequency does not change over the entirety of the 24-hour period, suggesting that the sensor did not pick up on any minute environmental changes

which would drastically change its resonance frequency, a characteristic that would be particularly useful for the purposes of this sensor.

b. Sensor Response to Temperature

Figure 2 and Figure 3 shows sensor response to changes in temperature, measured in °C. The temperature range for this experiment was 32°C to 42°C. Physiological body temperature typically ranges between 36.5°C to 37.5°C so the temperature range used contained all normal physiological temperatures (Osilla, 2023). Figure 2 shows that the resonance frequency stays constant throughout all temperatures in this range for all sensors within this experiment. However, the quality factor (Q factor) does vary throughout this experiment, as shown in Figure 3. This suggests that the resonance frequency is not sensitive to changes in temperature, but the Q factor is and thus can help monitor changes in temperature. This is expected because change to resonance frequency will be minimal with capacitance and inductance not being influenced highly by the changing temperature. Thermal expansion is minimal in the same 10°C temperature range which would contribute very little to capacitance and resistance changes.

c. Sensor Response to Different Fluids (PBS vs mSBF)

Figure 4 shows sensor response to mineral deposition via 4x modified simulated body fluid (4x mSBF) and phosphate-buffered saline (PBS) over a 24-hour period of time. Over the course of the 24-hour period, the resonance frequency decreased by 6.9% due to the deposition of minerals on the sensor surface. The plateau observed in Figure 4 after the first 5 hours of the experiment is due to the mineral deposition also plateauing. Since the vial only contains 10 mL of 4x mSBF, it also has a limited amount of salts within that volume of 4x mSBF that can deposit onto the surface of the sensor. That amount is very limited and comes out of solution within the first few

hours, eventually plateauing which is seen in the resonance frequency of the sensor. The variance of the sensor's resonance frequency seemingly moving between two different frequencies in the latter time points is indicative of noise from the environment causing the resonance frequency to shift. Combined with the results from the temperature and PBS control tests, these results indicate that the LC sensor is sensitive to mineral deposition onto the sensor surface and that changes in other parameters do not affect the resonance frequency.

d. Ongoing Work

The experiments mentioned in this thesis are preliminary experiments to test the design and sensing mechanism of the current LC sensor design. Having characterized the response of the sensor to various test parameters, future work will focus on testing the LC sensor in increasingly more physiologically similar environments, foremost of which includes introducing cells. While mSBF can replicate the general crystalline structure of the apatite structure of bone, it does not contain any cells which will provide a new challenge to the sensor's sensing mechanism.

VI. BIBLIOGRAPHY

American Board of Orthopaedic Surgery. (2019, January 31). *What is Orthopaedics?*. ABOS. https://www.abos.org/about/what-is-orthopaedics/

Baino, F., & Yamaguchi, S. (2020). The Use of Simulated Body Fluid (SBF) for Assessing Materials Bioactivity in the Context of Tissue Engineering: Review and Challenges. *Biomimetics (Basel, Switzerland)*, *5*(4), 57. https://doi.org/10.3390/biomimetics5040057.

Types of Orthopedic Implants. Center for Orthopaedic Surgery & Sports Medicine. (2019, November 8). https://www.centerfororthosurgery.com/types-of-orthopedic-implants/

Huang, Q.-A., Dong, L., & Wang, L.-F. (2016). Passive Wireless Sensors Toward a Wireless Sensing Platform: Status, Prospects, and Challenges. *Journal of Microelectromechanical Systems*, *25*(5), 822–841. https://doi.org/10.1109/jmems.2016.2602298.

Karipott, S. S., Veetil, P. M., Nelson, B. D., Guldberg, R. E., & Ong, K. G. (2017). An embedded wireless temperature sensor for orthopedic implants. *IEEE Sensors Journal*, 1–1. https://doi.org/10.1109/jsen.2017.2780226.

Karipott, S. S., Nelson, B. D., Guldberg, R. E., & Ong, K. G. (2018). Clinical potential of implantable wireless sensors for orthopedic treatments. *Expert Review of Medical Devices*, *15*(4), 255–264. https://doi.org/10.1080/17434440.2018.1454310.

Khan, Md. R., An, T. K., & Lee, H. S. (2021). A battery-free, chipless, highly sensitive LC pressure sensor tag using PEDOT: PSS and melamine foam. *IEEE Sensors Journal*, *21*(2), 2184–2193. https://doi.org/10.1109/jsen.2020.3021076

LC Circuits. LC circuits. (n.d.). https://web.pa.msu.edu/courses/2000fall/phy232/lectures/accircuits/lccircuits.html

Liu, S., Broucek, J., Virdi, A. S., & Sumner, D. R. (2011). Limitations of using micro-computed tomography to predict bone–implant contact and mechanical fixation. *Journal of Microscopy*, *245*(1), 34–42. https://doi.org/10.1111/j.1365-2818.2011.03541.x

Ong, K. G., Grimes, C. A., Robbins, C. L., & Singh, R. S. (2001). Design and application of a wireless, passive, resonance-circuit environmental monitoring sensor. *Sensors and Actuators A: Physical*, *93*(1), 33–43. https://doi.org/10.1016/s0924-4247(01)00624-0

Osilla, E. V. (2023, July 30). *Physiology, temperature regulation*. StatPearls [Internet]. https://www.ncbi.nlm.nih.gov/books/NBK507838/

S. M. Kurtz, E. Lau, H. Watson, J. K. Schmier, and J. Parvizi, "Economic burden of periprosthetic joint infection in the United States," *J. Arthroplasty*, vol. 27, no. 8, pp. 61–65.e1, 2012.

Tan, C. P., & Craighead, H. G. (2010). Surface Engineering and patterning using parylene for biological applications. *Materials*, *3*(3), 1803–1832. https://doi.org/10.3390/ma3031803

Torstrick, F. B., Safranski, D. L., Burkus, J. K., Chappuis, J. L., Lee, C. S. D., Guldberg, R. E., Gall, K., & Smith, K. E. (2017). Getting PEEK to Stick to Bone: The Development of Porous PEEK for Interbody Fusion Devices. *Techniques in orthopaedics (Rockville, Md.)*, *32*(3), 158–166. https://doi.org/10.1097/BTO.0000000000000242.